Laterally Dispersing Nozzles for Needle-assisted Jet Injection

James W. McKeage, Nandoun Abeysekera, Bryan P. Ruddy, *Member, IEEE,* Poul M. F. Nielsen, *Member, IEEE* Andrew J. Taberner, *Senior Member, IEEE*

***Abstract*— Most transdermal drug delivery systems are designed to inject drugs through the skin in a direction normal to the skin surface. However, in some drug delivery applications, such as local anesthesia, it is desirable to disperse the drug in a direction parallel to the surface of the skin. In this paper we present nozzles for needle-assisted jet injection that are designed to laterally disperse the fluid drug at a chosen depth in tissue. These nozzles were manufactured by laser machining holes in the walls of 0.57 mm (24 gauge) hypodermic needles, and sealing the end of the needle. An existing controllable jet injection system was used to test the nozzles. High-speed video recordings were taken to examine the shape of the high-speed jets emitting from the orifices, and jet injections into post mortem porcine tissue were performed to evaluate the resulting dispersion pattern. These injections demonstrated the ability of these nozzles to achieve a widely spread dispersion at a depth of 3 mm to 4 mm in tissue. We observed that the widest dispersion occurred at the same depth as the orifices, and dispersion was greater in the direction of the jets. Further investigation, including an in vivo study, is now required to evaluate whether this technique can improve the dispersion of anesthesia resulting from a single injection.**

I. INTRODUCTION

Jet injection is a transdermal drug delivery technique that forms a fluid drug into a high speed jet in order to deliver it through the skin. The key advantage of this technique is that it removes the need for a needle, and thus avoids the associated drawbacks of needle stick injury, needle misuse, and needle phobia [1]. However, as well as avoiding the use of a needle, jet injection can also result in a significantly dispersed pattern of delivery within the tissue relative to delivery with a needle. This has possibly contributed to some studies finding that jet injection can result in an improved immune response to vaccines [2]–[4], and different time profiles of anesthetic onset, and duration, relative to a needle based delivery [5]–[8]. The potential advantages associated with the dispersion of a jet injected liquid have led to the investigation of 'needle-assisted' jet injection [9]. This technique uses a small needle to pierce through the tough epidermal layer and allows significantly reduced pressures and jet speeds subsequently required to perform an injection.

Our previous work in needle-assisted jet injection demonstrated that this technique could be used to deliver a liquid drug deep into tissue (~12 mm) from the tip of ~2 mm syringe needle [9]. This outcome prompted us to trial a variation of this concept where, rather than attempting to achieve greater depth of penetration, we instead disperse the fluid more widely at a constant depth. If similar delivery characteristics to that presented by [9] could be achieved when delivering the drug laterally under the skin, it would result in a much more widely spread dispersion pattern. This could be very beneficial in areas such as the transdermal delivery of local anesthetic, where surgeons must typically infiltrate the anesthetic very slowly, over many injections sites, to anesthetise a large area of tissue. This process prolongs operations, adds to cost, and is painful for patients, with multiple needle pricks and injections required to adequately distribute the local anaesthetic across a large surface area.

In this work we present novel needle-assisted jet injection nozzles designed to deliver the drug laterally underneath the skin. These orifices are tested using an existing laboratory jet injection system capable of highly controlled jet speed profiles. High speed videography is used to observe the shape of the jets produced by the orifices, and initial injections into post mortem porcine tissue are presented to demonstrate the delivery pattern resulting from the use of these lateral delivery injection nozzles.

II. METHODS

A. Nozzle Fabrication

Two needle-assisted jet injection nozzles were produced, a two-orifice and a four-orifice nozzle (Fig. 1). In both nozzles the orifices were evenly spaced around the circumference of a 0.57 mm (24 G) hypodermic needle, approximately 5 mm from the needle tip. The orifices were laser micromachined into the walls of the needles using a femtosecond pulsed laser system (τ = 30 fs, repetition rate = 500 Hz, λ = 800 nm) with single pulse energies of 172 μJ. Needles were mounted on a 3-axis translation stage and the laser beam was focused at the

This work was supported by the MedTech Centre of Research Excellence (grant number #3505716), funded by the Tertiary Education Commission of New Zealand; and the Science for Technological Innovation National Science Challenge (grant number CRS-S3-2016), funded by the New Zealand Ministry of Business, Innovation and Employment.

J. W. McKeage and N. Abeysekera are with the Auckland Bioengineering Institute, University of Auckland, Auckland, New Zealand (james.mckeage@auckland.ac.nz; nandoun.abeysekera@auckland.ac.nz).

B. P. Ruddy, P. M. F. Nielsen, and A. J. Taberner are with the Auckland Bioengineering Institute and the Department of Engineering Science, University of Auckland, Auckland 1142 New Zealand (email: b.ruddy@auckland.ac.nz; p.nielsen@auckland.ac.nz; a.taberner@auckland.ac.nz)

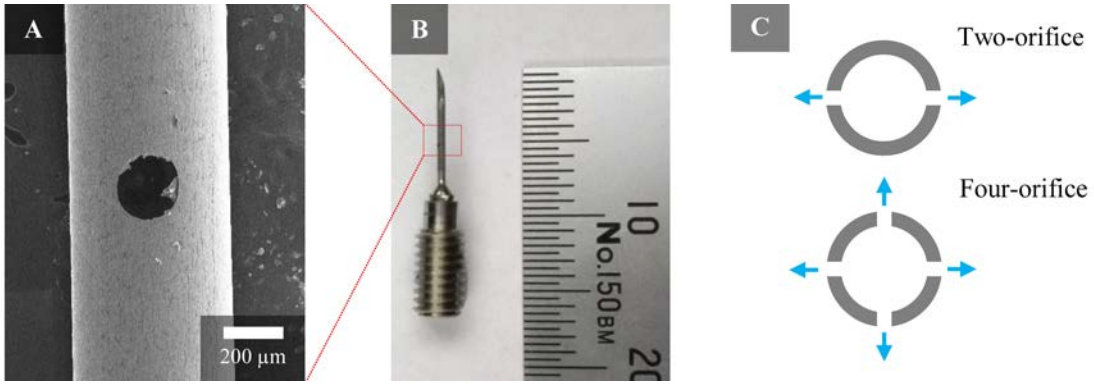

Figure 1 - A) Scanning electron microscope image of one of the laser machined orifices in the wall of the 24 gauge needle. B) Photograph of the needle soldered in the stainless steel insert, the needle continues approximately 2 mm into the insert. C) Diagram of a slice through the needle at the point of the machined orifices, indicating the difference between the two nozzles used in this study.

central axis of the needle using an 80 mm focusing objective. Holes were generated by translating the needle in a circular path, allowing the laser to machine through both faces of the needle. The laser was translated around the previously described circular path seven times. The orifices in the two-orifice nozzle had areas of $3.50 \times 10^{-8}\,m^2$ and $3.95 \times 10^{-8}\,m^2$, while those in the four-orifice nozzle were $1.40 \times 10^{-8}\,m^2$, $1.43 \times 10^{-8}\,m^2$, $2.56 \times 10^{-8}\,m^2$ and $2.62 \times 10^{-8}\,m^2$.

The needle tip was sealed with solder to ensure that fluid was only ejected from the lateral orifices. The needles were cut to a length of approximately 10 mm and mounted within stainless steel inserts (O'keefe Controls Co).

B. Injection System

The nozzles were used with an existing controllable jet injection system, previously presented in [10]. This system was driven by a voice coil motor (BEI Kimco LA30-75) which actuates a stainless-steel piston within a 5.62 mm diameter ampoule with a maximum volume of 1.4 mL. A potentiometer (Omega LP803) was used to record the position of the motor throughout the injection. A volumetric average of the jet speed was computed from this measurement of position.

A field programmable gate array (FPGA) chassis (NI-9114, National Instruments) and real-time controller (NI-9024) were used to control the voice coil actuator. Software to interact with this system was developed in LabVIEW 2011, and included a position control loop operating at 20 kHz. The control strategy for this device involved a combination of feedforward, and feedback control [11]. The feedforward model predicts the voltage required to achieve the desired jet speed, while the feedback control allows the system to respond to small disturbances, and make minor adjustments to ensure the desired speed is achieved. The drive signal for this system was developed within the LabVIEW software and amplified by a pair of linear power amplifiers (AE Techron 7224). Further details regarding this injection system, and its control, can be found in [10].

C. Experimentation

1) System Characterisation

A series of step voltage measurements were performed to calibrate the feedforward control model for these nozzles. Voltages steps from 0 V to 80 V were applied to the motor and the resulting steady state coil speed, and volumetric jet speed were recorded. A 3rd order polynomial was fit between the results, providing an estimate of the voltage required to achieve the desired speed. With the feedforward model calibrated, position setpoint profiles based on the desired jet speed and volume could be produced to achieve the desired injection. The measurement of actual position relative to the setpoint was used to observe the ability of the control system to achieve the desired speed and volume.

2) High-speed Video

High speed videos were recorded during ejections of water (60 m/s) into air in order to observe the shape of the jets produced by these orifices. A video of each nozzle was obtained using a high speed camera (Phantom Micro LC 110) recording at a rate of 2000 frames per second.

3) Porcine Tissue Injections

Porcine abdominal tissue was used as an in vitro model of human tissue to evaluate the delivery characteristics of the orifices. This tissue was harvested post mortem from animals approximately 12 weeks of age in accordance with the University of Auckland Code of Conduct for the Use of Animals for Teaching and Research. The tissue was frozen at −80 °C until required for testing, at which time it was thawed to room temperature. Once thawed the porcine tissue was cut into 30 mm by 30 mm samples. Each sample received one injection at a jet speed of 100 m/s, and total volume of 0.3 mL. Six injections, three with each nozzle, were performed with a solution of dye (0.1 % Brilliant Blue FCF, Queen Fine Foods Pty. Ltd.) in water. These samples were frozen immediately after injection, then, once frozen, sectioned to observe the location of the dye in the tissue. This sectioning was performed down two orthogonal planes in the tissue. In the case of the two-orifice nozzle these planes were through the axis of the jets, and perpendicular to the jet axis. In the case of the four-orifice injections, the two planes aligned with the two orthogonal axes of the jets.

In two further tissue injections a solution of iodine based contrast agent was delivered (0.647 kg/L iohexol, Omnipaque 300), rather than dye. Following injection these two samples were placed in a micro-CT scanner (Bruker Skyscanner 1172), and a 360 degree scan was performed. The x-ray source was set to a voltage of 85 kV and current of 118 µA. This scan produced images of 666 pixels by 1000 pixels, with a pixel size of 27.4 µm. These images were reconstructed into a 3D volume using the *NRecon* software package.

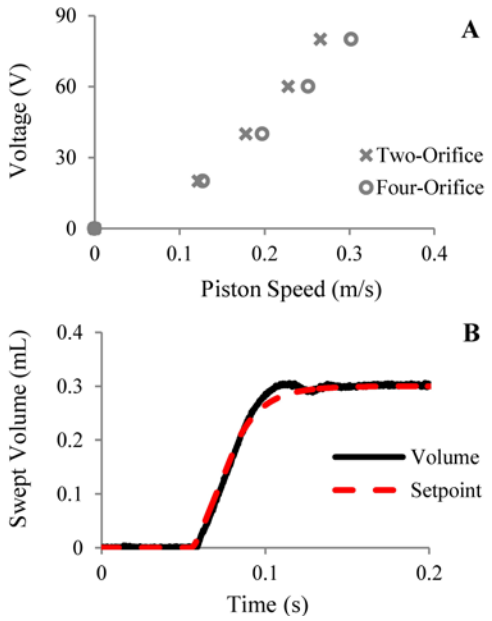

Figure 3 - A) The measured Voltage versus Coil Speed relationship used to inform the feedforward model. B) An example injection where the system was asked to deliver 0.3 mL at 100 m/s.

Images of the sections produced from the dye injections, and the results of the micro-CT injections, were used to measure the width of dispersion at its widest point in the tissue. This was done by manually selecting, and measuring, the widest point of dispersion at a constant depth using the *ImageJ* software package [12].

III. Results

A. System Characterisation

The measured steady state piston speeds during the step inputs of voltage up to 80 V are shown for both nozzles in Fig. 2A. This information allowed the feedforward controller to output the correct voltage for the desired jet speed. Fig. 2B shows an example of a controlled injection where 0.3 mL was delivered at 100 m/s with the two-orifice nozzle. In this plot the measured position follows the desired setpoint closely, indicating the injection system has achieved the desired jet speed and volume.

B. High-speed Video

Fig. 3 shows selected images from the high speed videos produced with each nozzle, the full videos can be accessed in [13]. The videos demonstrate that the two-orifice nozzle produces two jets in opposite directions, while the four-orifice nozzle produces four jets each 90° apart. All six jets produced by these two nozzles demonstrate a very divergent jet shape.

C. Micro-CT

Fig. 4 shows results from the reconstructed volumes of the porcine tissue samples which were injected, then scanned in the micro-CT. These results include central slices through the reconstructed volume, and images of the delivered contrast agent segmented from the surrounding tissue. The two-orifice injection shows that wider dispersion has been achieved in the directions of the jets, relative to the orthogonal plane. Both these samples demonstrate the sponge-like or channel-network dispersion pattern in the subcutaneous fat that has been observed in previous studies [9], [14].

D. Porcine Tissue Injections

Example images of tissue samples that were injected with dye, then sectioned, are shown in Fig. 5. The maximum width at a constant depth was measured from images such as these. For the two-orifice nozzle the average maximum width was 14.5 mm ± 1.8 mm in the direction of the jets, while it was 9.8 mm ± 1.0 mm orthogonal to the jet axis. In the case of the four-orifice nozzle the maximum width in the direction of one pair of jets was 9.3 mm ± 2.5 mm, while it was 10.2 mm ± 1.7 mm in the other plane. The depths at which these maximum widths were observed were 4.2 mm ± 0.5 mm and 3.2 mm ± 0.8 mm for the two-orifice and four-orifice nozzles, respectively.

IV. Discussion

The results presented here demonstrate the ability of these laser machined, needle-assisted jet injection nozzles to produce laterally dispersing injections. The high speed videos showed the jets were produced only at the laser machined orifices, with no leaks around the needle or through the solder

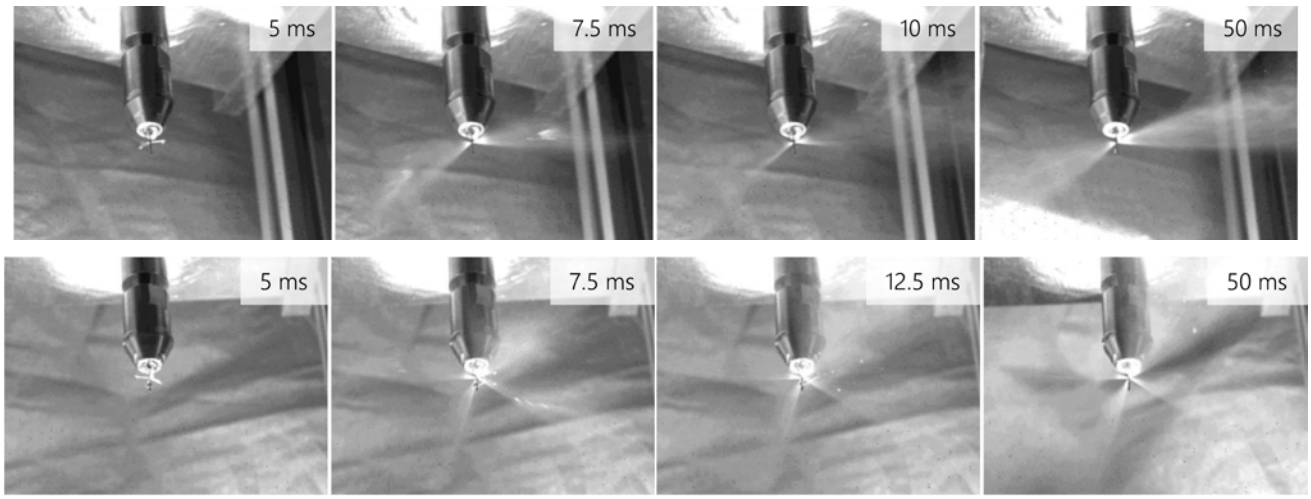

Figure 2 - Selected frames from the high speed videos of the two-orifice (top) and four-orifice injection nozzles. The full videos can be accessed here: https://auckland.figshare.com/s/71f3fae667cf715d7946 [12].

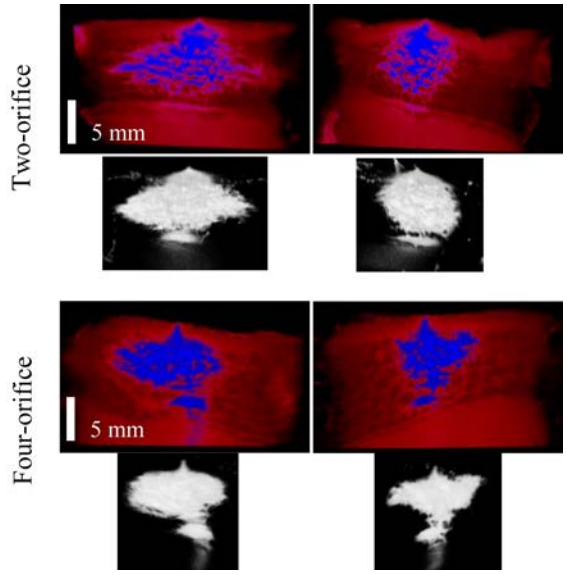

Figure 5 - Results from the reconstructed 3D samples imaged using a micro-CT scanner. The top images are slices through the centreline of the samples where the colour has been adjusted to represent the injected fluid as blue and tissue as red. The lower images are of the injected bolus segmented out of the surrounding tissue. The view angle of the bolus is intended to match that of the slice directly above it.

block in the end of the needle. The initial tissue experiments presented in this work showed that the use of these nozzles results in a bolus of drug deposited at the approximate depth of the orifices, but dispersing approximately 3 mm to 4 mm into the tissue. As expected, dispersion in the direction of the jets was greater than that in the perpendicular direction for injections with the two-orifice nozzle, while the width of dispersion was largely similar in the two orthogonal jet axes of the four-orifice nozzle. In some samples dispersion was significantly deeper than the depth of the orifices. This was likely due to the orifices being positioned 5 mm away from the needle tip, so some fluid was able to follow the path of the needle and reach much greater depths in the tissue (Fig. 5). The 5 mm distance was chosen for ease of manufacture, and should be minimised in future to avoid this effect.

Previous injection studies have usually been more focused on measuring depth rather than radial dispersion; hence there is a paucity of measurements to which to compare our findings. However, it is clear that some jet injection studies have achieved lateral dispersion comparable to that observed here [10], [15]. The extent and depth at which this lateral dispersion occurs has been quite variable in jet injection studies, so it is promising to observe that, with the needle-assisted nozzles presented here, the depth of maximum spread, and the axes of spread, coincide with the location of the orifices.

Delivery patterns similar to that observed in these results have also been observed in previous jet injection studies [10], [16] and even in previous work with needle assisted jet injection [9]. 'Elliptical' dispersion patterns were described by [9] where their needle-assisted injector penetrated around 2 mm into the tissue before producing a ~50 m/s jet which penetrated a further 6 mm to 7 mm into the subcutaneous fat. Despite using a greater jet speed (100 m/s), the needle assisted injections in this paper penetrated, on average, just 5.4 mm.

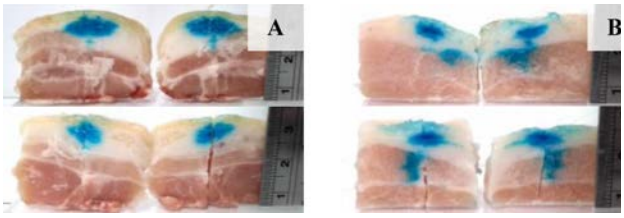

Figure 4 - Two samples that have been injected with blue dye, frozen, then sectioned. The left sample has been injected using the two-orifice nozzle, while the right used the four-orifice nozzle. The sample on the right also provides an example of the unintended deeper delivery caused by the needle penetrating 5 mm deeper than the orifices.

This could possibly be due to the difference in jet shape as the jets presented here are very divergent, while the injections by [9] involved a collimated jet. A recent study has shown that a collimated jet will penetrate significantly further than one that is divergent [17], so perhaps it would be preferable to develop much more collimated jets with a needle-assisted nozzle to achieve greater dispersion areas in the tissue.

The key motivation for this work is the delivery of local anesthetic to the nerves in the subdermal plexus. Jet injection of anesthetic has been trialed in many previous studies, and has been shown to produce anesthesia of the target region [1], [6]. Given these previous results, it is reasonable to expect that delivery patterns such as those shown in Fig. 4 and Fig. 5 would have produced successful anesthesia of the skin had they been delivered to in vivo tissue. However, some of the previous studies delivering anesthetic by jet injection indicate that jet injected anesthetic has an increased onset time [7], [8], or a shorter duration of anesthesia [5], [6] relative to needle based delivery. It will be important to investigate how well this lateral needle-assisted jet injection results in anesthesia, and evaluate whether this approach can anesthetise a larger area of tissue.

V. Conclusions

Laser-machined holes in the walls of two hypodermic needles were used to produce laterally dispersing needle-assisted jet injection nozzles. These nozzles were used with an existing controllable jet injection setup to perform injections. High speed videography demonstrated that these nozzles formed jets of a very divergent shape. Injections into porcine tissue demonstrated that wide dispersion was achieved at the depth of the orifices, with the widest spread occurring in line with the jets. Further investigation should now be conducted to evaluate the ability of this technology to result in more widely spread anaesthesia.

VI. References

[1] S. Mitragotri, "Current status and future prospects of needle-free liquid jet injectors," *Nat. Rev. Drug Discov.*, vol. 5, no. 7, pp. 543–548, Jul. 2006.

[2] J. Williams, L. Fox-Leyva, C. Christensen, D. Fisher, E. Schlicting, M. Snowball, S. Negus, J. Mayers, R. Koller, and R. Stout, "Hepatitis A vaccine administration: comparison between jet-injector and needle injection," *Vaccine*, vol. 18, no. 18, pp. 1939–1943, Mar. 2000.

[3] J. C. Aguiar, R. C. Hedstrom, W. O. Rogers, Y. Charoenvit, J. B. Sacci, D. E. Lanar, V. F. Majam, R. R. Stout, and S. L. Hoffman, "Enhancement of the immune response in rabbits to a malaria DNA vaccine by immunization with a needle-free jet device," *Vaccine*,

vol. 20, no. 1–2, pp. 275–280, 2001.

[4] G. Kersten and H. Hirschberg, “Needle-free vaccine delivery,” pp. 459–474, 2007.

[5] C. Makade, P. Shenoi, and M. Gunwal, “Comparison of acceptance, preference and efficacy between pressure anesthesia and classical needle infiltration anesthesia for dental restorative procedures in adult patients,” *J. Conserv. Dent.*, vol. 17, no. 2, p. 169, 2014.

[6] A. C. A. de Oliveira, K. de S. Amorim, E. M. do Nascimento Júnior, A. C. B. Duarte, F. C. Groppo, W. M. Takeshita, and L. M. de A. Souza, “Assessment of anesthetic properties and pain during needleless jet injection anesthesia: a randomized clinical trial,” *J. Appl. Oral Sci.*, vol. 27, no. 0, p. e20180195, Jan. 2019.

[7] M. Hajimaghsoudi, E. Vahidi, M. Momeni, A. Arabinejhad;, and M. Saeedi, “Comparison of local anesthetic effect of lidocaine by jet injection versus needle infiltration in lumbar puncture,” *Am. J. Emerg. Med.*, 2016.

[8] B. Saghi, M. Momeni, M. Saeedi, and M. Ghane, “Efficacy of the jet injector in local anaesthesia for small wound sutures: A randomised clinical trial compared with the needle infiltration technique,” *Emerg. Med. J.*, vol. 32, no. 6, pp. 478–480, 2015.

[9] X. Li, B. Ruddy, and A. Taberner, “Characterization of needle-assisted jet injections,” *J. Control. Release*, vol. 243, pp. 195–203, 2016.

[10] J. W. McKeage, B. P. Ruddy, P. M. F. Nielsen, and A. J. Taberner, “The effect of jet speed on large volume jet injection,” *J. Control. Release*, vol. 280, pp. 51–57, 2018.

[11] A. Taberner, N. C. Hogan, and I. W. Hunter, “Needle-free jet injection using real-time controlled linear Lorentz-force actuators,” *Med. Eng. Phys.*, vol. 34, no. 9, pp. 1228–1235, 2012.

[12] K. Eliceiri, C. A. Schneider, W. S. Rasband, and K. W. Eliceiri, “NIH Image to ImageJ : 25 years of image analysis HISTORICAL commentary NIH Image to ImageJ : 25 years of image analysis,” *Nat. Methods*, vol. 9, no. 7, pp. 671–675, 2012.

[13] J. McKeage, “High Speed Video of Lateral Needle-assisted Jet Inejction,” *Figshare*, 2019. [Online]. Available: https://auckland.figshare.com/s/71f3fae667cf715d7946. [Accessed: 18-Feb-2019].

[14] K. Comley and N. Fleck, “Deep penetration and liquid injection into adipose tissue,” *J. Mech. Mater. Struct.*, vol. 6, no. 1–4, pp. 127–140, Jun. 2011.

[15] J. Baxter and S. Mitragotri, “Jet-induced skin puncture and its impact on needle-free jet injections: Experimental studies and a predictive model,” *J. Control. Release*, vol. 106, pp. 361–373, 2005.

[16] J. Schramm-Baxter and S. Mitragotri, “Needle-free jet injections: Dependence of jet penetration and dispersion in the skin on jet power,” *J. Control. Release*, vol. 97, pp. 527–535, 2004.

[17] G. Park, A. Modak, N. C. Hogan, and I. W. Hunter, “The effect of jet shape on jet injection,” *Proc. Annu. Int. Conf. IEEE Eng. Med. Biol. Soc. EMBS*, vol. 2015–Novem, pp. 7350–7353, 2015.